Fish tracking in vertical slot fishways using computer vision techniques

Álvaro Rodríguez, María Bermúdez, Juan R. Rabuñal and Jerónimo Puertas

ABSTRACT

Vertical slot fishways are hydraulic structures which allow the upstream migration of fish through obstructions in rivers. The appropriate design of these devices should take into account the behavior and biological requirements of the target fish species. However, little is known at the present time about fish behavior in these artificial conditions, which hinders the development of more effective fishway design criteria. In this work, an efficient technique to study fish trajectories and behavior in vertical slot fishways is proposed. It uses computer vision techniques to analyze images collected from a camera system and effectively track fish inside the fishway. Edge and region analysis algorithms are employed to detect fish in extreme image conditions and Kalman filtering is used to track fish along time. The proposed solution has been extensively validated through several experiments, obtaining promising results which may help to improve the design of fish passage devices.

Key words | computer vision, fish behavior, tracking, vertical slot fishway

Álvaro Rodríguez (corresponding author)
Department of Information and Communications Technologies,
Faculty of Informatics,
University of A Coruña,
Campus de Elviña s/n 15071, A Coruña,
Spain
E-mail: *arodriguezta@udc.es*

María Bermúdez
Jerónimo Puertas
Department of Hydraulic Engineering, ETSEC,
University of A Coruña,
Campus de Elviña s/n 15071, A Coruña,
Spain

Juan R. Rabuñal
Centre of Technological Innovation in Construction and Civil Engineering (CITEEC),
University of A Coruña,
Campus de Elviña s/n 15071, A Coruña,
Spain

INTRODUCTION

The construction of water resources management works, such as dams, weirs, water diversions, and other barriers, leads to significant changes in the river ecosystem. These structures constitute a physical barrier to fish natural movements, which negatively impacts their populations. In fact, this interruption of free passage has been identified as the main reason for the extinction or the depletion of numerous species in many rivers (Jackson *et al.* 2001).

One of the solutions to restore longitudinal connectivity of rivers is the construction of fishways, vertical slot fishways being a common and widely used type (Figure 1). These devices basically consist of a channel with a sloping floor that is divided by baffles into a series of pools. Water runs downstream in this channel through a vertical slot from one pool to the next one below. The hydraulic characteristics of vertical slot fishways vary according to the geometric dimensions and configuration of the pools and baffles and have been studied by both numerical and physical modeling (Rajaratnam *et al.* 1986; Puertas *et al.* 2004; Tarrade *et al.* 2008; Bermúdez *et al.* 2010; Chorda *et al.* 2010).

At the same time, several authors have examined fish swimming capabilities (Dewar & Graham 1994; Blake 2004) and found evidence that fish are confronted by a challenging hydrodynamic environment when they swim upstream vertical slot fishways. However, these works are generally carried out in experimental flumes, in which flow features differ significantly from those found in vertical slot fishways, and little is known about fish behavior in these particular artificial conditions. Besides, very few works have studied the interaction between the biological and physical processes that are involved in swimming upstream a vertical slot fishway (Puertas *et al.* 2012). Consequently, it is necessary to develop new methodologies to analyze fish behavior in these devices, which in turn will contribute to the establishment of more effective fishway design criteria.

doi: 10.2166/hydro.2014.034

Figure 1 | Full-scale vertical slot fishway model used in this study. Photo taken at CEDEX (Center for Studies and Experimentation of Public Works, Madrid, Spain).

One of the main difficulties in studies of fish passage is that the existing mechanisms to measure fish behavior, such as direct observation or placement of sensors on the specimens, are impractical or seriously affect the fish behavior (Castro-Santos *et al.* 1996). In this context, techniques based on the use of imaging and acoustic information can constitute an important alternative. Acoustic transmitters or scanners and video cameras have been used to observe fish for some time (Armstrong *et al.* 1992; Steig & Iverson 1998). In recent works, computer vision techniques have been used in applications such as fish tracking in a tank using color contrast and fluorescent marks (Duarte *et al.* 2004) or fish recognition in clear water by color properties and background subtraction (Chambah *et al.* 2004).

Considering a wider perspective, different authors have used image processing techniques to detect, count, or track fish. These works use techniques such as stereo vision (Petrell *et al.* 1997), background models (Morais *et al.* 2005), shape priors (Clausen *et al.* 2007), local thresholding (Chuang *et al.* 2011), moving average algorithms (Spampinato *et al.* 2008), particle image velocimetry techniques (Deng *et al.* 2004), pattern classifiers applied to the changes measured in the background (Lines *et al.* 2001), or artificial neural networks (ANN) (Rodriguez *et al.* 2011). Finally, some techniques based on infrared imaging (Baumgartner *et al.* 2010) or laser imaging detection and ranging technologies (Mitra *et al.* 2006) can also be found in the literature. Recently, these technologies have been integrated with Kalman filtering techniques to improve fish tracking. In Shortis *et al.* (2013) they were applied to monitor fish recorded with stereo imaging devices, whereas in Jensen & YangQuan (2013) they were used to locate fish tagged with radio transmitters.

However, it should be noted that most of the published techniques have been carried out in calm water conditions and with controlled light sources and therefore are not suitable to be used inside a fishway. In addition, some of these techniques use marks or light sources, which may influence fish behavior, while others employ special and expensive sensors, which may only be used at certain points of the structure.

This work proposes a technique to analyze fish behavior in vertical slot fishways, which is intended to complete the fishway design methodology with experimental results. In each test, living fish are introduced into a fishway model equipped with an overhead camera system, and fish trajectory and behavior are studied by means of computer vision techniques. The method can provide researchers with valuable information about fish–structure interaction, such

as fish resting areas and times, fish velocities and accelerations, or passage success rates. As well, the results can be used to formulate and calibrate models that predict fish movement behavior (Weber *et al.* 2006). This may ultimately contribute to improving the efficiency of these types of devices.

This work continues the research started in Rodriguez *et al.* (2011), in which the camera acquisition system and the methodology to conduct the experiments are described. In this previous paper, a new technique combining image processing and ANN is proposed to automatically detect fish in the images. In this case, only preliminary results were obtained and experimental tests were carried out with a single fish species. Also, the resulting accuracy was not compared with that of other techniques.

This paper focuses on improving the image analysis techniques to detect and track fish in a fishway. To this end, a new and more efficient technique is proposed, based on the combination of region and edge analysis. This technique replaces the ANN described in Rodriguez *et al.* (2011) which, although providing satisfactory results, was found to be slower and less accurate. Also, a new procedure based on the extended Kalman filter was integrated in the technique to effectively track fish in the presence of image occlusions or in a multiple fish scenario. It uses probabilistic analysis to compare detected and predicted fish positions and allows the separation of different trajectories and removal of anomalous detections.

Finally, several extensive experiments have been conducted to support the conclusions of this work, using 259 individuals of four fish species and different light and flow conditions. In total, the technique is applied to about 500 millions of images recorded in 15 assays performed from 2010 to 2012.

PROPOSED TECHNIQUE

The proposed technique detects and tracks fish in a vertical slot fishway, analyzing the images acquired with a multicamera system. It uses a combination of computer vision techniques and processes the information to obtain different parameters regarding the interaction between fish and fishway.

The technique has been tested in a full-scale fishway model, located at the CEDEX (Center for Studies and Experimentation of Public Works in Madrid, Spain), which consists of a 20 m long, 1.5 m wide, and 1 m deep flume (Figure 1). It contains 11 pools, with the geometric dimensions detailed in Figure 2. The slope of the fishway during the tests was 7.5% and the total discharge was set to 250 L/s.

The camera system consists of 28 cameras with fisheye lenses, placed in the fishway in an overhead perspective and partially submerged. The seven upper pools are covered (four cameras have been installed in each pool, as shown in Figure 3) and turbulence and surface reflections are avoided. The cameras are integrated into a monitoring and data acquisition system, which is described in detail in Rodriguez *et al.* (2011).

The main steps of the proposed technique can be summarized as follows:

(1) camera calibration: the image distortion is eliminated and a projective model is designed to integrate measurements from the different cameras into a common coordinate space;
(2) segmentation: a dynamic background model of the scene is created and subtracted from the image to highlight regions where the fish can be found. A technique based on the combination of region and edge analysis is then applied to detect fish;
(3) representation and interpretation: the detected objects are translated into a descriptive representation which can be operated with. A first filtering step is done at this point;
(4) tracking: the detected objects are used as the input of a filter extended from the Kalman model. This is an algorithm that uses a motion model and works in a similar way to a Bayesian filter. It allows the deletion of isolated noise detections, separation of different

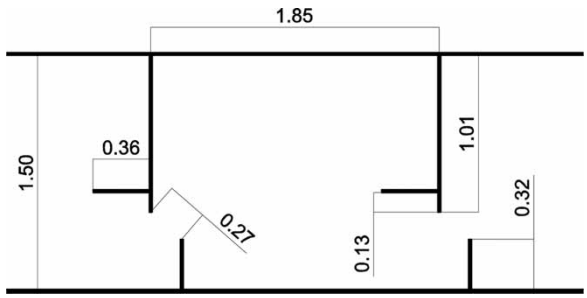

Figure 2 | Dimensions of a pool in the physical model (in meters).

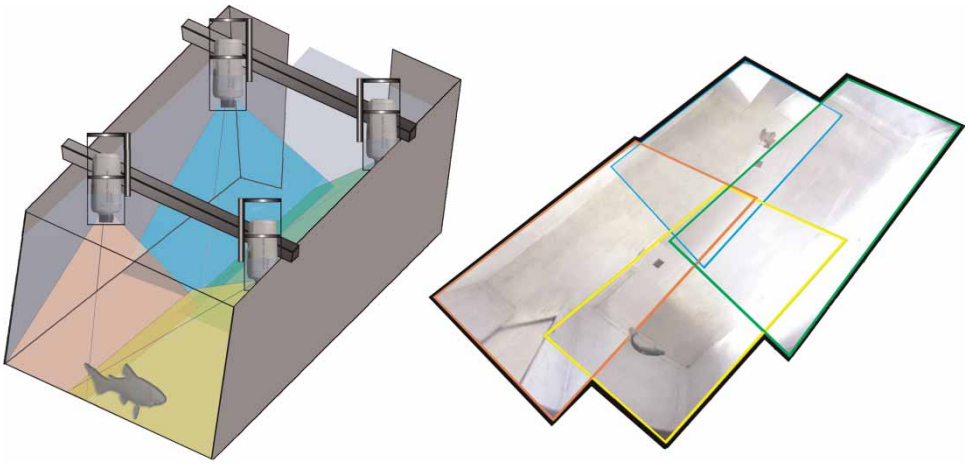

Figure 3 | Image acquisition scheme and camera overlapping (left). Example of a fishway pool formed with the projected images from four cameras (right). Each polygon represents the field of a different camera.

fish, estimation of hidden positions, and prediction of next positions;

(5) filtering: a filtering process is performed on the obtained fish trajectory in order to overcome artifacts in the detections and to ensure a soft trajectory;

(6) data processing: the data are integrated with hydraulic information and processed to calculate the output information, such as fish velocities or accelerations.

Camera calibration

The first step of the algorithm is to calculate the transformation from coordinates in a particular camera to real coordinates in the fishway. This is performed in two stages: first, the parameters to correct and scale the image are obtained for each camera; second, the transformation of each camera into a common coordinate system is calculated.

For the first stage, we use the pin-hole projective model (Zhang 1999) which describes how a point from the real space is projected into the image plane, as shown in Figure 4. Pin-hole equations can be written as follows:

$$\begin{bmatrix} x_i \\ y_i \\ 1 \end{bmatrix} = M \times \begin{bmatrix} x_c \\ y_c \\ 1 \end{bmatrix} \quad M = \begin{bmatrix} f_x & 0 & c_x \\ 0 & f_y & c_y \\ 0 & 0 & 0 \end{bmatrix} \tag{1}$$

where (x_i,y_i) are the coordinates of the point in the image and (x_c,y_c) are the projected coordinates in space. M is called transformation matrix and is defined by the focal

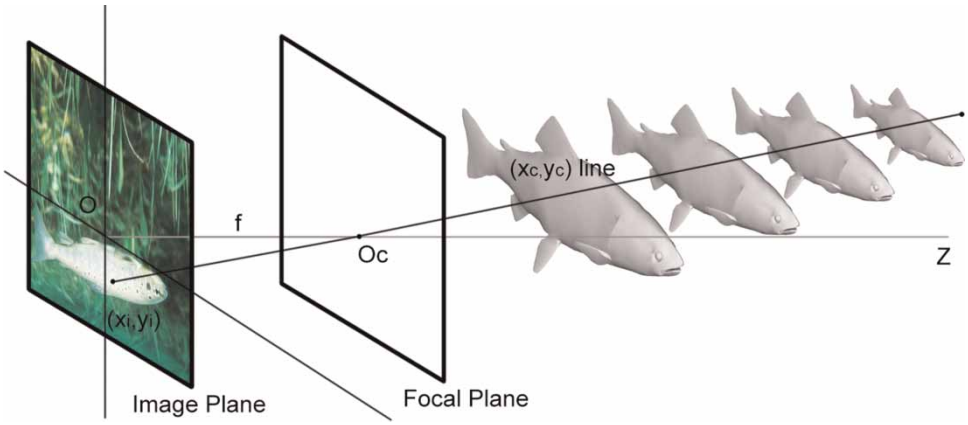

Figure 4 | Pin-hole camera model. Projection of a point onto the image plane in an ideal camera.

length $f = (f_x, f_y)$ and the principal point $O = (c_x, c_y)$, which is the projection of the center of the lens or optical center O_c onto the image plane.

In practice, the previous model needs to be extended, due to the distortions and defects of the lenses (Weng *et al.* 1992). The influence of distortion is modeled using the following equations:

$$x_c = x_d(1 + k_1 r^2 + k_2 r^4 + k_3 r^6) + 2p_1 x_d y_d + p_2(r^2 + 2x_d^2)$$
$$y_c = y_d(1 + k_1 r^2 + k_2 r^4 + k_3 r^6) + p_1(r^2 + 2y_d^2) + 2p_2 x_d y_d \quad (2)$$

where (x_c, y_c) and (x_d, y_d) are the distorted and undistorted coordinates of the point, respectively, k_i are the radial distortion parameters coefficients, p_i are the tangential distortion coefficients, and r represents the distance from the distorted coordinates to the principal point.

To obtain the matrix M and the distortion coefficients k_i and p_i, the real geometry of a calibration pattern is compared with the geometry observable in the images of the pattern. The parameters of the model are solved using the technique proposed in Zhang (1999), minimizing the reprojection error with the Levenberg-Marquardt optimization algorithm. In this way, the coordinates of the point in the real space (X, Y, Z) are calculated from the coordinates of the point in the image (x_i, y_i), taking into account $x_c = X/Z$ and $y_c = Y/Z$ for a given Z. In this work, the Z value was calculated assuming that the average distance between the fish and the bottom is 5 cm. The underlying assumption is that the fish swim preferentially near the bottom of the flume, which was verified in preliminary experimental tests and is consistent with observations made in similar studies (Mateus 2007; Silva *et al.* 2012; Branco *et al.* 2013).

In addition, the refraction of light in the water must be considered. Thus, cameras should be calibrated underwater or refraction should be modeled with an additional transformation. In this case, an affine model is employed to perform this task.

In the second process, the measurements obtained by each camera are projected to a common coordinate system, the entire pool being covered. Thus, applying an equation of general projective geometry, the transformation M_2 between the global coordinate space d' and the coordinate space d, obtained from a specific camera, can be expressed as follows:

$$\begin{bmatrix} x_{d'} \\ y_{d'} \\ 1 \end{bmatrix} = M_2 \times \begin{bmatrix} x_d \\ y_d \\ 1 \end{bmatrix} \quad M_2 = \begin{bmatrix} a & b & c \\ d & e & f \\ g & h & i \end{bmatrix} \quad (3)$$

To solve the equation above, a number of visual marks have been placed in the areas where the vision field of the cameras overlaps (Figure 3).

Segmentation

Image segmentation is the process of dividing an image into multiple parts, in this case, with the aim of separating the fish from the background. Every segmentation algorithm addresses two problems: the criteria for a good partition and the method for achieving an efficient one (Yilmaz *et al.* 2006). In statistics, this problem is known as cluster analysis and is a widely studied area with hundreds of different algorithms (Szeliski 2011).

Therefore, it is first necessary to find a variable or group of variables (features) which allow a robust separation of the fish from the background, as well as to choose a classification technique according to the selected variables. This problem requires analysis of the distinctive visual properties of the fish and the background (Cheng *et al.* 2001; Zhang *et al.* 2008).

At present, the most common criteria to detect fish in images are based on color features and *a priori* knowledge of the background. However, these techniques do not perform well in underwater images, even for calm water and high quality images, due to the low levels of contrast (Lines *et al.* 2001). Besides, acquired images in this study will be characterized by extreme luminosity changes and huge noise levels, making texture and features based on *a priori* color properties useless.

Taking this into account, different techniques are considered in this work. They are detailed in the Results section and provide a comparative framework for evaluating the system performance. These techniques involve a two-step process. First, the variability of the images is reduced using knowledge of the background. Second, an adaptive analysis is performed either on the discontinuities of the

image (edge-based classification) or on the local similarity of pixels (region-based classification). Owing to the need to operate the system by non-experts, only non-supervised techniques have been considered and, given the huge amount of images to be analyzed, computational complexity was decided as being a critical factor.

One of these techniques, previously developed in Rodriguez *et al*. (2011), consists of a self-organizing map (SOM) neural network (Kohonen 1982). The SOM model is aimed at establishing a correlation between the numerical patterns supplied as an input and a two-dimensional output space (topological map). This characteristic can be applied to image segmentation and SOM networks have been widely used in the image analysis field (Ahmed & Farag 1997; Verikas *et al*. 1997; Waldemark 1997; Ngan & Hu 1999; Dong & Xie 2005). Although promising results were obtained in this early work (Rodriguez *et al*. 2011), the SOM approach requires more computational time compared to more straightforward techniques, such as the ones proposed in this paper. Besides, the SOM technique depends on the training patterns selected.

In this work, a combination of two simple techniques is selected, together with an image preprocessing procedure and a dynamic background modeling, to overcome the limitations of the SOM approach. The first selected technique is a modern implementation of the Canny edge detector, which proved to be less noisy than other edge-finding methods such as the Sobel or the Prewitt operators. Edges corresponding to the frontiers between fish and background are obtained by means of four directional filters which detect horizontal, vertical, and diagonal discontinuities in the derivatives of the images (Canny 1986).

To reduce the false positives obtained, the objects detected by the edge analysis are filtered using a second segmentation technique. This second technique is the Otsu method, which performs a region classification by automatically thresholding the image histogram. It is a fast and efficient technique to separate dark objects in a white background (Sezgin & Sankur 2004). The final outcome will include only the objects detected by the edge algorithm which overlap 95% with those found with the region technique.

To include knowledge about the background in the method, a dynamic background is calculated forming a synthetic image. Before the application of the segmentation technique, the image is normalized and the foreground is extracted using this background model. This procedure is known in computer vision as background subtraction.

The synthetic background is constructed dynamically to handle light and long-term scene changes. It is calculated according to the following equation:

$$\mathrm{BI}_i(x, y) = 0.5 \times \mathrm{BI}_{i-1}(x, y) + 0.5 \times I_i(x, y) \quad (4)$$

where I_i is the current processed image, corresponding to the frame i of the video, BI_i is the new background image, and BI_{i-1} is the previous background image. For $i = 1$ the background model is initialized using an image from the camera with no fish.

To update the background image along time, BI_{i-1} and I_i images are divided into four regions which are considered separately. Each region of the background image BI_{i-1} is updated with the current image I_i if no objects were detected and if time elapsed from the previous update exceeds a certain value (which was empirically set by default to 30 frames).

To enhance the image quality, the images are preprocessed using a standard contrast-limited adaptive histogram equalization technique. Also, the borders where the waterproof cases of the cameras produced a black region (without information) were masked.

Representation and interpretation

As a result of the segmentation process, the image is divided into different regions representing background and possible fish. At this point, it is possible to use a higher level processing, adding knowledge extracted from the characteristics of real fish, to interpret the segmented image. To this end, the objects detected in the previous step are translated into convenient descriptors, which can be used to perform different operations: its area, its centroid (calculated as the average position of the body pixels), and the minimum ellipse containing the body.

Subsequently, an algorithm classifies each detected body into fish or non-fish categories. The operation of this algorithm is divided in three stages, as shown in Figure 5. In the first stage, the detected bodies are discarded or classified as either fish or small bodies. To this end, a shape criterion

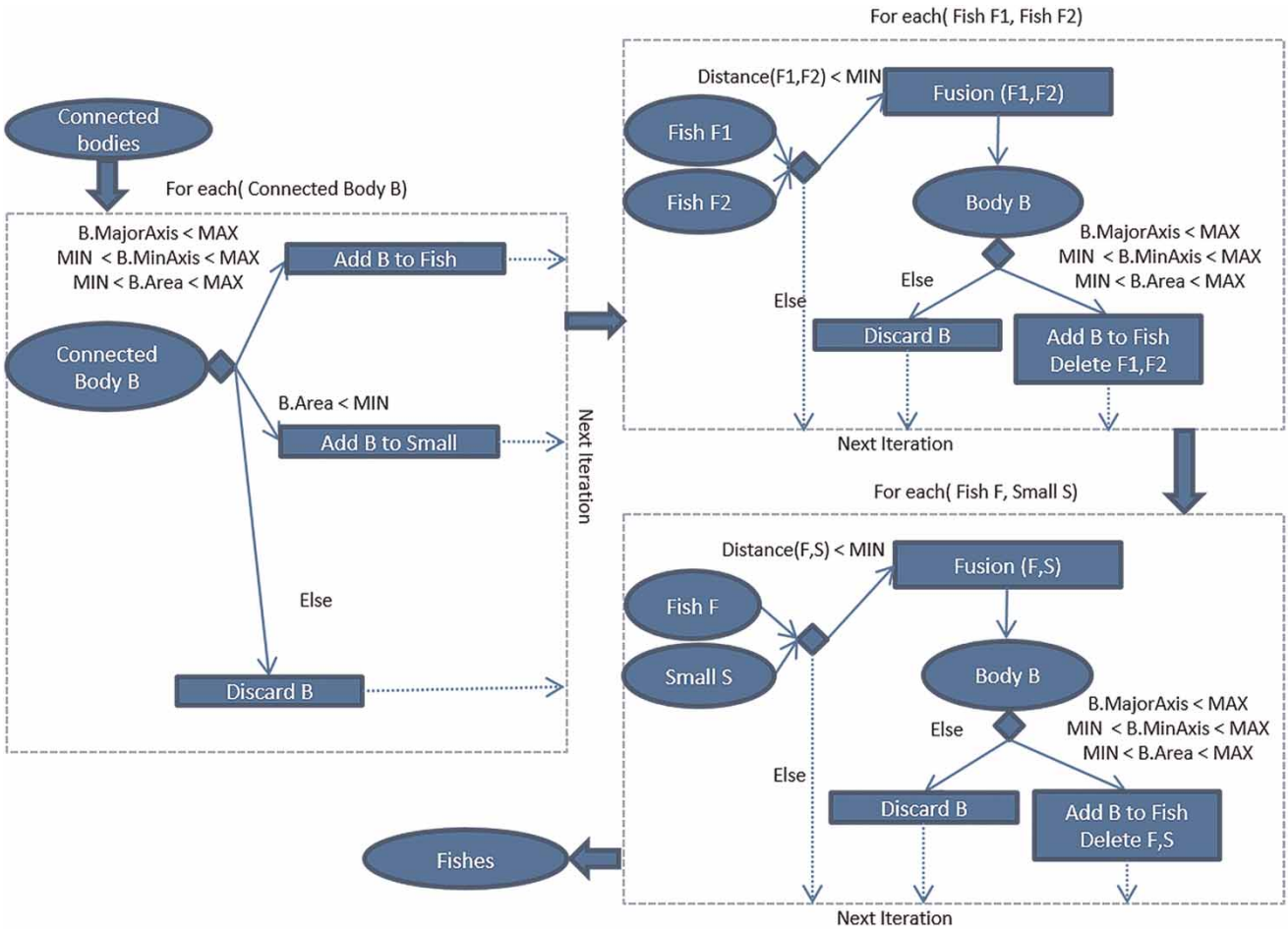

Figure 5 | Diagram of the algorithm used to interpret the segmented image.

based on value ranges of the above descriptors is defined for each fish species. In the second stage, close fish bodies are joined if the resulting body verifies the shape criterion. Finally, small bodies are either joined with detected fish or discarded. Figure 6 shows the obtained results when applying image interpretation.

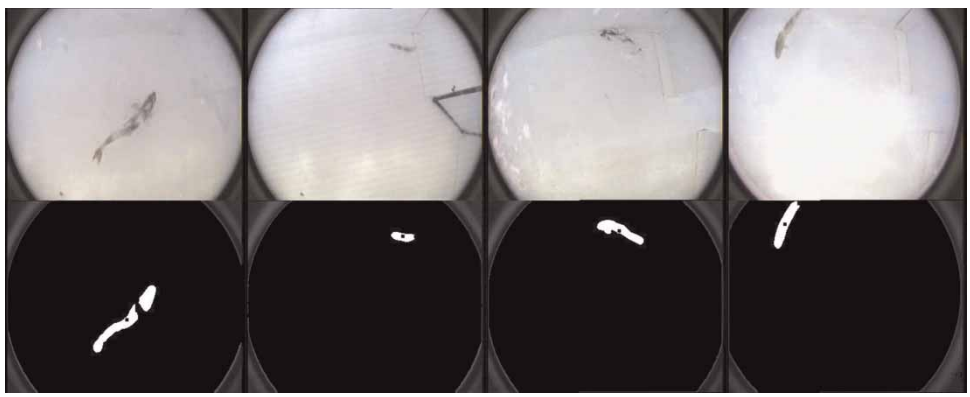

Figure 6 | Results obtained after representation and interpretation of the segmented image. Original images are shown at the top of the figure and processed images at the bottom. Each detected body is marked in white and each fish center is marked with a small dark square. Note that some bodies have been interpreted as parts of the same fish.

Tracking

Tracking is the problem of generating an inference about the motion of one or more objects from a sequence of images. It can be solved using several approaches, including motion estimation and feature matching techniques. Some of the most important approaches consider a statistical point of view and formulate the problem as a prediction correction process based on Bayesian theory.

A well-known technique in this group is the Kalman filter, which has been selected in this work (Stenger *et al.* 2001; Arulampalam *et al.* 2002; Yu *et al.* 2005; Yun & Bachmann 2006; Gift & Paulin 2014). It addresses the problem of estimating the state $x \in R^n$ of a discrete-time controlled process that is governed by the linear stochastic difference equation, expressed as follows:

$$x(t+1) = Ax(t) + w(t) \tag{5}$$

where A is a $n \times n$ matrix called state transition matrix, which relates the state of the system at the previous time step to the state at the current step, and w represents the process noise, which is assumed normally distributed with mean 0.

For the state transition matrix, we consider the equations of two-dimensional motion assuming a constant acceleration between time steps

$$\begin{aligned} x_{t+1} &= x_t + v_{xt} + \frac{1}{2}a_x \\ y_{t+1} &= y_t + v_{yt} + \frac{1}{2}a_y \\ v_{xt+1} &= v_{xt} + a_x \\ v_{yt+1} &= v_{yt} + a_y \end{aligned} \tag{6}$$

where (x,y) is the fish position, (v_x,v_y) is the velocity, and (a_x,a_y) is the acceleration, which is assumed constant in a time step (equal to the frequency of the image acquisition, i.e., 0.04 s).

We also consider an observation model described by the following equation:

$$z(t) = Hx(t) + v(t) \tag{7}$$

where $z \in R^m$ represents the measurement, H is a $m \times n$ matrix called observation matrix, and v is the measurement error, which is assumed independent of w and normally distributed with mean 0.

After the calibration process, it is assumed that real world positions can be inferred from observed positions in the image. So the model equations can be expressed as follows:

$$\begin{bmatrix} x_{t+1} \\ v_{xt+1} \\ a_{xt+1} \\ y_{t+1} \\ a_{yt+1} \\ v_{yt+1} \end{bmatrix} = \begin{bmatrix} 1 & 1 & 0 & 0 & 0 & 0 \\ 0 & 1 & 1 & 0 & 0 & 0 \\ 0 & 0 & 1 & 0 & 0 & 0 \\ 0 & 0 & 0 & 1 & 1 & 0 \\ 0 & 0 & 0 & 0 & 1 & 1 \\ 0 & 0 & 0 & 0 & 0 & 1 \end{bmatrix} \begin{bmatrix} x_t \\ v_{xt} \\ a_{xt} \\ y_t \\ a_{yt} \\ v_{yt} \end{bmatrix} + w(t)$$

$$\begin{bmatrix} z_x \\ z_y \end{bmatrix} = \begin{bmatrix} 1 & 0 & 0 & 0 & 0 & 0 \\ 0 & 0 & 0 & 1 & 0 & 0 \end{bmatrix} \begin{bmatrix} x_t \\ v_{xt} \\ a_{x,t} \\ y_t \\ a_{yt} \\ v_{yt} \end{bmatrix} + v(t) \tag{8}$$

The Kalman filter works in a two-step recursive process. First, it estimates the new state, along with their uncertainties. Once the outcome of the next measurement (corrupted with noise) is observed, these estimates are updated using a weighted average. The higher weight is given to the estimates with higher uncertainty. The algorithm can, therefore, run in real time using only the current input measurements and the previously calculated state. In the present work, the implementation of the Kalman filter was performed according to Welch & Bishop (2006), obtaining an empirical estimate of the measurement error and the process noise covariances.

The Kalman filter is designed to track multiple objects, which are referred to as fish or tracks. The essential problem which is solved at this point is the assignment of detections to fish. To associate detections to tracks, a cost is assigned to every possible pair of fish–detection. The cost is understood as the probability of that detection to correspond to the current fish position. It is calculated using the distance from the detected position to the predicted position and to the last confirmed position of the fish. To this end, the minimum of the Euclidean distances is selected as cost metric.

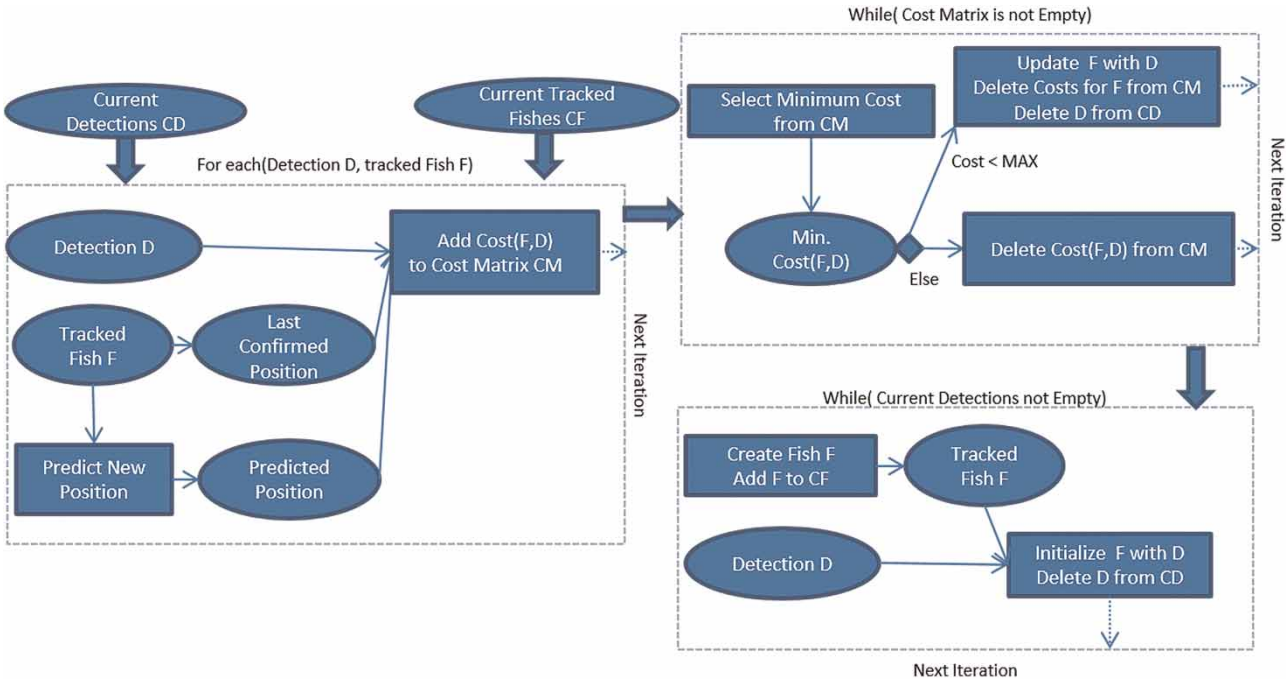

Figure 7 | Diagram of the algorithm used to assign detections to fish.

Therefore, every detection is assigned to the track with the lower cost, provided that it is lower than a selected value and each track can only be assigned to one detection. When a new detection is assigned to a fish, the predicted position for that instant is confirmed and corrected. Detections which remain unassigned to any existing fish are assumed to belong to new tracks. In addition, if a fish remains unassigned for too long, its track is closed, so no new assignments can be made to that fish. Fish without enough detections are assumed to be noise and deleted. The operation of the assignment algorithm is described in the schematic of Figure 7 and the results obtained in a situation with two fish are shown in Figure 8. In conclusion, this technique does not only obtain trajectories from detections, but also allows filtering some of the false positives of the system and estimating the fish position when it is not detected in the images.

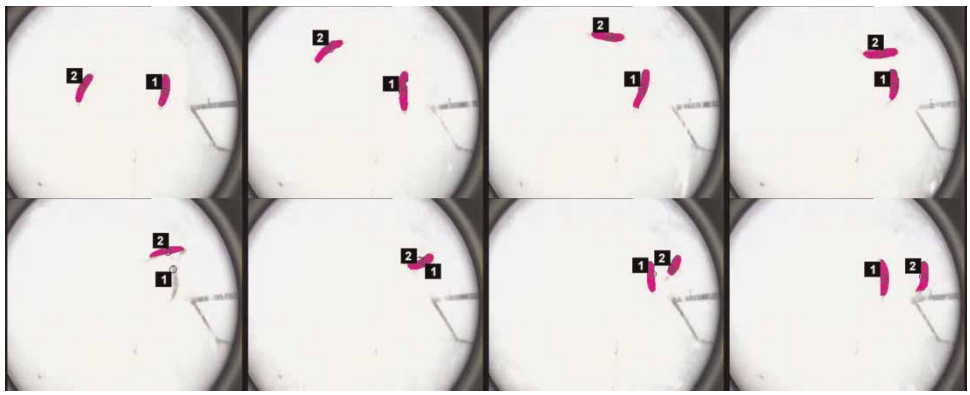

Figure 8 | Results obtained with the Kalman filter in a sequence of images, ordered from left to right and from top to bottom. Fish detections are shown as gray areas superimposed to the images. Black circles and labels indicate tracked fish. Note that the position of the two fish is calculated even if they are not detected in the image.

Filtering

The result of the process so far is the position vector of every detected fish along time, representing its full trajectory in the fishway. However, these results are still expected to show certain undesirable phenomena caused by the small variability of the calculated position of the centroid, the parts of fish which are hidden by bubbles, and the errors in perspective and alignment of planes, when the fish moves from one camera's field of view to another.

To solve these problems and to remove some of the noise still present in the results, a complex filtering process is required. First, the relative position of the cameras is taken into account to solve differences between simultaneous observations. Thus, when the fish is detected simultaneously by two or more cameras, its position is the average of all the observed positions. To determine whether two observations from different cameras belong to the same target, the trajectories resulting from the Kalman filter are compared. If they start and end in adjacent cameras at similar times, they are then merged. When more than one fish crosses simultaneously from one camera field of view to another, the distance from the last predicted position in the old camera to the first position in the new camera is used as a cost function.

In the next step, a moving average filtering process is applied (SIGMUR 2003) and outliers are detected by thresholding the distance between filtered and original positions. Therefore, while normal detections are simply replaced by their filtered ones, the outliers are substituted by the average of the previous and next confirmed detections. This implies that predicted positions near outliers are no longer valid and they are hence replaced using interpolation techniques.

Data processing

As the result of the previous process, the fish position in the fishway over time is obtained. From the fish position vector, the observed instantaneous velocities are calculated as follows:

$$\bar{v}_{\text{obs}} = \left(\frac{X_i - X_{i-1}}{t_i - t_{i-1}}, \frac{Y_i - Y_{i-1}}{t_i - t_{i-1}} \right) \tag{9}$$

where X_i and Y_i are the x and y coordinates of the fish in the global coordinate system in time t_i, and $\bar{v}_{\text{obs}}$ is the observed fish velocity vector.

However, the observed velocities are not really those which quantify the real effort made by fish to swim. To calculate the actual swimming velocities, the water velocity in the pools is taken into account as follows:

$$\bar{v}_{\text{swim}} = \bar{v}_{\text{obs}} - \bar{v}_{\text{flow}} \tag{10}$$

where $\bar{v}_{\text{swim}}$ is the fish swimming speed vector and $\bar{v}_{\text{flow}}$ is the flow velocity vector.

As noted above, the water velocity in the fishway can be evaluated by means of experimental studies or numerical models. In this case, the velocity field in the pools was computed with a numerical model based on the two-dimensional depth averaged shallow water equations. The experimental validation of this model in 16 different fishway designs, as well as a detailed description of the model equations, can be found in Bermúdez *et al*. (2010).

Once the fish swimming velocities are known, their accelerations $\bar{a}_i$ are calculated according to the following expression:

$$\bar{a}_i = \left(\frac{v_{\text{swim}x,i} - v_{\text{swim}x,i-1}}{t_i - t_{i-1}}, \frac{v_{\text{swim}y,i} - v_{\text{swim}y,i-1}}{t_i - t_{i-1}} \right) \tag{11}$$

where $v_{\text{swim}x}$ and $v_{\text{swim}y}$ are the x component and the y component of the fish swimming velocity.

In addition, further information regarding fish behavior can be obtained from the analysis of the trajectory and the times spent in the fishway. On one hand, fish response to physical factors such as current velocity or turbulence levels can be studied and preferential fish paths and areas for rest can be determined. On the other hand, total ascending times, which are an important component of passage delay, can be calculated. In this line, resting times, passage success, and total distances covered can be also examined. Although further research is needed, the analysis of these parameters can contribute to the definition of key factors in fish passage through these devices. In this way, the need to provide specific resting zones or to keep the velocity and turbulence levels below a certain threshold can strongly affect the fishway design.

RESULTS

Accuracy of the system

To measure and compare the accuracy of the system, several experiments were performed in a full-scale vertical slot fishway model located in the CEDEX laboratory. From these experiments, a data set was created to apply the proposed technique and other well-known methods. The data set is composed of 135 videos with a total of 11,028 images, corresponding to different cameras, pools, and fishway regions, as well as different daylight conditions and fish species. These videos were manually labeled by experts who marked on the images the fish center positions and this information served as ground-truth to evaluate the techniques. To measure the accuracy, the precision and recall metrics were used

$$\begin{aligned} \text{Precision} &= \frac{\text{true positive}}{\text{true positive} + \text{false positive}} \\ \text{Recall} &= \frac{\text{true positive}}{\text{true positive} + \text{false negative}} \\ \text{False positive rate} &= 1 - \text{precision} \\ \text{False negative rate} &= 1 - \text{recall} \end{aligned} \tag{12}$$

As aforementioned, the techniques published so far have been carried out in calm water or with controlled light conditions. They are generally based on visual marks or specific sensors and cannot be applied in the context of this work. Thus, to compare the proposed technique with other algorithms, some widely used non-supervised segmentation approaches have been implemented and tested by means of the previous metrics.

Specifically, the following techniques have been used:

- Region: a region segmentation algorithm based on the Otsu method;
- Edge: a modern implementation of the Canny edge detector;
- Edge–region: a combination of the two previous techniques. It is the one proposed in this paper;
- SOM pix: a SOM neural network based on the RGB intensity values of the image from the neighborhood of each pixel;
- SOM avg: a SOM neural network in which input is the local average of the RGB values in a window centered in the neighborhood of the pixel;
- SOM feat: a SOM neural network that uses two different image features: the local average of the RGB values in a window centered in the neighborhood of the pixel and the standard deviation of the RGB values in the column and file of the pixel.

Three different versions of each technique were implemented: one without background information and another two in which a background is used to normalize the image. In the latter case, either a static frame without fish or the proposed dynamic background technique was used to model the background. In every case, images were enhanced with a standard contrast-limited adaptive histogram equalization technique.

When using the SOM techniques, a three-layer topology with three processing elements (neurons) in each layer was selected and a 3×3 window was used for each input. To mitigate the dependence of the results on the selected training patterns, all networks were trained using three different data sets. In addition, the SOM network proposed in Rodriguez *et al.* (2011) was considered in the comparative.

The results obtained after the representation and interpretation step for the different techniques are shown in Table 1. It can be observed that the results are strongly dependent on the background model. Only the proposed technique performed well without background modeling and, in general, dynamic background achieved better results than the static one.

It can also be noted that the worst results in terms of accuracy are obtained with the edge technique. On the other hand, SOM models based on features achieve good accuracy, but require a higher computational time. Finally, although the region technique obtained quite good results, the proposed technique yielded the same level of precision with the best recall, without increasing significantly the execution time.

Once the representation and interpretation step is completed, fish detections are processed with the tracking algorithm. As explained above, this algorithm can operate as a filter, using the confirmed positions of the tracked fish. The results obtained using this configuration are

Table 1 | Accuracy of the selected techniques after representation and interpretation step

Average results	Precision	Recall	False pos. rate	False neg. rate	Time (s/frame)
No background					
SOM pixel	0.43	0.29	0.57	0.71	1.38
SOM avg.	0.55	0.35	0.45	0.65	3.60
SOM feat.	0.63	0.26	0.37	0.74	11.63
Edge	0.86	0.73	0.14	0.27	0.34
Region	0.40	0.39	0.60	0.61	0.40
Edge–region	0.93	0.71	0.07	0.29	0.31
Static background					
SOM pixel	0.91	0.49	0.09	0.51	1.55
SOM avg.	0.96	0.72	0.04	0.28	3.41
SOM feat.	0.96	0.62	0.04	0.38	11.22
SOM (Rodriguez *et al.* 2011)	0.85	0.69	0.15	0.31	3.37
Edge	0.65	0.75	0.35	0.25	0.35
Region	0.94	0.81	0.06	0.19	0.19
Edge–region	0.94	0.82	0.06	0.18	0.32
Dyn. background					
SOM pixel	0.96	0.78	0.04	0.22	1.15
SOM avg.	0.96	0.61	0.04	0.39	11.62
SOM feat.	0.96	0.72	0.04	0.28	3.61
Edge	0.67	0.78	0.33	0.22	0.32
Region	0.95	0.78	0.05	0.22	0.17
Edge–region (proposed)	0.95	0.82	0.05	0.18	0.31

shown in Table 2. Techniques without background have been discarded, as they generally achieved low accuracy.

However, the tracking technique can also estimate hidden positions of the fish. This is done by the Kalman algorithm, which predicts fish locations based on the motion model (Equation (6)). Following this procedure, the results include both confirmed and estimated positions (Table 3).

The precision of the system is increased significantly if the algorithm operates only as a filter. However, the use of predicted positions improves the recall, without losing precision when compared to the results before the tracking step (Table 1).

It must be taken into account that some of the new false positives that appear when using predictions are not errors.

Table 2 | Accuracy of the selected techniques with background modeling after tracking and filtering steps. Only confirmed detections are used

Average results	Precision	Recall	False pos. rate	False neg. rate	Time (s/frame)
Static background					
SOM pixel	0.97	0.81	0.03	0.19	1.14
SOM avg.	0.98	0.74	0.02	0.26	3.71
SOM feat.	0.97	0.64	0.03	0.36	11.97
SOM (Rodriguez *et al.* 2011)	0.88	0.75	0.12	0.25	3.27
Edge	0.70	0.83	0.30	0.17	0.33
Region	0.97	0.84	0.03	0.16	0.18
Edge–region	0.97	0.84	0.03	0.16	0.31
Dyn. background					
SOM pixel	0.97	0.80	0.03	0.20	1.15
SOM avg.	0.98	0.74	0.02	0.26	3.67
SOM feat.	0.97	0.63	0.03	0.37	11.87
Edge	0.75	0.85	0.25	0.15	0.33
Region	0.97	0.81	0.03	0.19	0.17
Edge–region (proposed)	0.98	0.85	0.02	0.15	0.31

Table 3 | Accuracy of the selected techniques with background modeling after tracking and filtering steps. Both confirmed and predicted detections are used

Average results	Precision	Recall	False pos. rate	False neg. rate	Time (s/frame)
Static background					
SOM pixel	0.93	0.91	0.07	0.09	1.14
SOM avg.	0.95	0.86	0.05	0.14	3.71
SOM feat.	0.93	0.80	0.07	0.20	11.97
SOM (Rodriguez *et al.* 2011)	0.73	0.88	0.27	0.12	3.27
Edge	0.44	0.93	0.56	0.07	0.33
Region	0.94	0.94	0.06	0.06	0.18
Edge–region	0.94	0.94	0.06	0.06	0.31
Dyn. background					
SOM pixel	0.94	0.91	0.06	0.09	1.15
SOM avg.	0.95	0.86	0.05	0.14	3.67
SOM feat.	0.94	0.80	0.06	0.20	11.87
Edge	0.48	0.93	0.52	0.07	0.33
Region	0.94	0.93	0.06	0.07	0.17
Edge–region (proposed)	0.95	0.94	0.05	0.06	0.31

In fact, they may reflect the position of the fish when it is not observable in the images and the fish center position has not been manually marked.

Overall, the proposed technique obtained the best accuracy of all tested algorithms. It achieved one of the lowest false positive rates, false negative rates, and execution times. Hence, the technique is considered to obtain reliable results: it detects the fish in most situations and finds their true positions with a high probability.

Tracking errors

As shown in the previous section, the proposed technique performs comparatively better than the other implemented methods, in terms of precision and recall. However, the ability of the algorithm not only to detect fish in images but also to generate trajectories from fish still has to be tested. In this section, the capability of the system to observe fish along time is studied, which implies measuring the efficiency in assigning detections to fish.

Although there is not a standard metric to perform this task, it can be measured by analyzing and counting tracking errors. From a general point of view, this type of error can be classified as follows:

- Type 1: the output trajectory of a detected fish contains isolated noise detections;
- Type 2: a fish is not detected and does not generate a trajectory;
- Type 3: a group of noise detections is classified as a new fish and a trajectory is generated for a non-existing fish;
- Type 4: two or more trajectories are created for a single fish. This can happen if a group of noise detections interfere with the trajectory of a tracked fish, or if a tracked fish is lost for a long period of time;
- Type 5: two or more fish interact during some time, causing occlusions and overlapping in the images. This results in the assignment of some of the detections to the wrong trajectory.

Type 1 errors are reflected as false positives in the results of Tables 1–3. On the other hand, Type 2 errors do not occur, in practice, since video sequences are long enough to ensure that every fish is detected. Besides, most errors of Type 5 are not visually observable by human operators, since they usually correspond to changes in the relative position of two or more fish when they are occluded by turbulence or bubbles. Under these conditions, fish are not visually distinguishable from each other. However, interaction among fish was barely observed in high-velocity areas and it does not affect the global analysis of fish behavior in resting zones.

Table 4 | Summary of the tracking test

Data set	Type 3 errors	Type 4 errors	Error rate (per 1,000 frames)
Single fish	7	0	0.15
Two fish	0	2	0.18

Finally, longer sequences are required to analyze Type 3 and Type 4 errors and two new data sets have been created for this purpose. The first data set consists of a long sequence of 46,000 frames with a single fish moving in only one pool. The second one contains 10 sequences of 1,000 frames each, where two fish interact in the same pool. The obtained results can be seen in Table 4. They show a very low error rate, with one tracking error every 5,000 frames or more. These results confirm that the proposed system is suitable for obtaining fish trajectories from recorded images.

Experimental results

The proposed system was applied to 15 assays conducted in the full-scale vertical slot fishway model located at the CEDEX laboratory (Figure 1). During the corresponding migration period, four different species (a total of 259 fish) were tested: Iberian barbel (*Luciobarbus bocagei*), Mediterranean barbel (*Luciobarbus guiraonis*), Iberian straight-mouth nase (*Pseudochondrostoma polylepis*), and brown trout (*Salmo trutta*), as shown in Figure 9. The recordings of each assay last approximately 12 hours and the recording frequency is 25 Hz.

Passage success, understood as the percentage of fish ascending the entire fishway, was evaluated by analyzing the fish full trajectory. The results were verified by means of passive integrated transponder tag technology and direct observation. Overall, passage success during the experiments was low, regardless of species, and varied considerably with fish size (Table 5). In general, larger individuals presented a higher rate of success in ascending

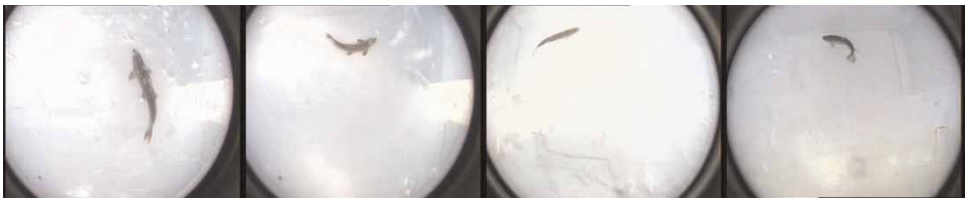

Figure 9 | Fish species used in the assays. From left to right: Iberian barbel, Mediterranean barbel, Iberian straight-mouth nase, and brown trout.

Table 5 | Overall passage success during the experiments

Species	Size (cm)	Number of fish	Passage success (%)
Iberian barbel	0–15	12	33.3
	15–20	12	75.0
	20–25	5	80.0
	>25	34	41.2
Mediterranean barbel	0–15	6	0.0
	15–20	8	0.0
	20–25	11	54.6
	>25	12	25.0
Iberian straight-mouth nase	0–15	61	9.8
	20–25	34	41.2
Brown trout	0–15	5	0.0
	15–20	43	14.0
	20–25	14	42.9
	25–30	2	100.0
Total		259	28.6

the entire fishway, relative to small specimens of the same species.

On the other hand, the path chosen by fish moving from one pool to another and the specific resting zones actually exploited by the fish were identified. In the experiments, the individuals avoided high-velocity areas and used recirculation regions, in which velocity and turbulence levels are lower, to move within the pool and for resting before ascending through the higher-velocity area of the slot. Thus, a preliminary analysis of the fish trajectories revealed that when ascending the fishway, fish spent the vast majority of time in low-velocity areas. Despite the high transit times observed occasionally in these areas, no signs of disorientation and very few fall back movements were detected in the recordings. This suggests that the use of resting zones influences fish passage delay, but not fishway passage success.

As noted above, fish rest frequently in low-velocity areas and, in fact, consecutive ascents of more than four pools (without a resting period) have not been observed. However, low-velocity areas were not frequented uniformly by fish, which stayed most frequently in the zone located just downstream from the slot and behind the small side baffle (zone A in Figure 10). The exploitation of low-velocity areas for the four species can be seen in Table 6. The frequency of use of resting zones is expressed as the proportion between the time spent in a specific one and the total resting time during the ascent. The results suggest that only the recirculation regions located in the upstream part of the pools (zones A and B) play an important role in fish passage. If these results are confirmed in further assays, designs in which zone C becomes a high-velocity area (examples can be found in Bermúdez *et al.* (2010)) would not be *a priori*

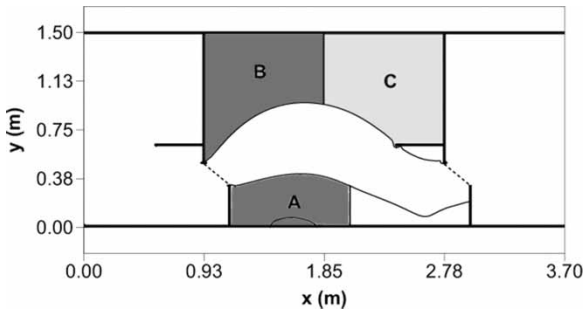

Figure 10 | Location of the resting zones considered in this work.

Table 6 | Exploitation of resting areas for the four species. The resting zones are labeled as in Figure 11

	Frequency of use (%)			
	A	B	C	Avg. resting time (s)
Iberian barbel	68.5	28.5	2.9	161
Mediterranean barbel	88.4	10.5	1.1	325
Iberian straight-mouth nase	99.8	0.0	0.2	269
Brown trout	82.7	16.7	0.6	1,271
Total	84.1	15.1	0.8	585

more unfavorable. Therefore, these results encourage the use of designs with low-velocity areas in the upstream part of the pools.

In addition, the paths taken by fish to swim from one pool to the next through the slot were analyzed separately. In general, two modes of successful ascents were observed, depending on the location of the individual within the pool before traversing the slot and the area used to approach it (Figure 11). The results suggest that all the selected fish species tend to follow similar trajectories and exploit the same flow regions during the ascent.

Finally, the observed speed, swimming speed, and acceleration have been calculated as described in the 'Data processing' section. Figure 12 shows a sample of obtained velocities and accelerations (in modulus), which are represented as a function of the traveled distance, and their respective polynomial fitting curves.

A clear trend is observed in fish swimming velocities, with a peak occurring immediately prior to crossing the slot and significant decrease in velocity once the fish passes to the next pool. This pattern is strongly influenced by the water velocities that fish are confronted by in the different regions of the fishway.

On the other hand, fish acceleration data are more scattered, being maximum accelerations observed when fish approach the slot. This is due to the fact that fish usually come from a resting area and need to reach a certain speed to traverse the slot. After crossing this high-velocity area, they usually decelerate.

Average maximum swimming speeds and accelerations can be seen in Table 7. Observed fish velocities are low relative to the flow velocity in the slot region, as shown in Figure 12. Hence, maximum swimming velocities are only slightly higher than the water velocity in the slot, regardless of the fish species.

Swimming velocities are usually defined as a function of fish body length (BL), since it is considered one of the most influential factors affecting speed (Beamish 1978). Figure 13 shows the maximum fish swimming velocities (v_{max}) obtained in the assays, expressed in BL/s. Differences between species are now observed, suggesting different levels of effort according to the sizes of the specimens. Obtained values do not exceed the maximum burst speed values proposed in the literature, which vary from 9 up to 15 BL/s (Weaver 1963; Webb 1975), 10 BL/s being the most accepted value (Cowx & Welcomme 1998).

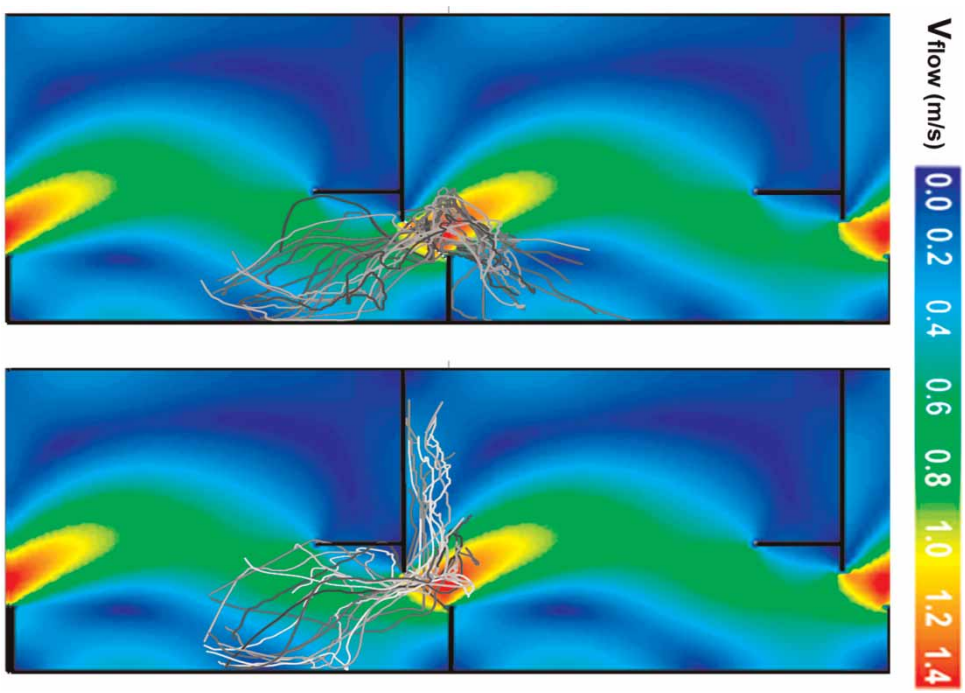

Figure 11 | Examples of the two typical fish swimming trajectories used to traverse a slot.

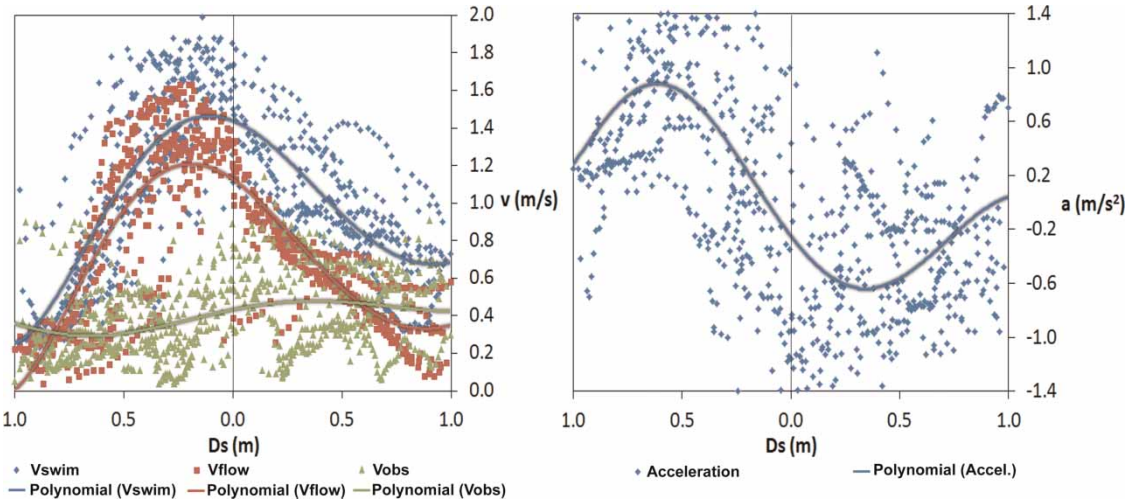

Figure 12 | Velocities and accelerations calculated for a set of pool ascents observed in the experimental tests. Ds is the traveled length from the slot section.

Table 7 | Average maximum swimming speeds and accelerations for the four species

	Swimming speed (m/s)		Acceleration (m/s^2)	
Species	**Avg. maximum**	**Std. deviation**	**Avg. maximum**	**Std. deviation**
Iberian barbel	1.51	0.27	1.13	0.60
Mediterranean barbel	1.51	0.25	0.95	0.60
Iberian straight-mouth nase	1.52	0.26	1.08	0.54
Brown trout	1.60	0.25	1.31	0.74

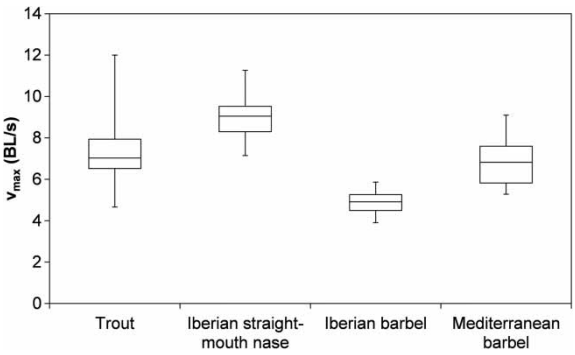

Figure 13 | Maximum fish swimming speeds expressed as a function of BL for the four species.

CONCLUSIONS

In this work, a new technique is developed to automatically analyze fish behavior in fishways. It uses several computer vision techniques to detect and track fish in video sequences recorded by a camera system integrated in the fishway.

More specifically, it employs a combination of background modeling, edge, and region analysis to detect fish. Also, it takes advantage of the Kalman filter to obtain the trajectory of one or multiple individuals inside the fishway.

The proposed technique has been extensively tested and compared with different standard methods. It achieved the best balance of precision, recall, and execution time.

In addition, the system was applied to 15 assays conducted during 2 years with more than 250 living fish. It provided valuable information regarding fish behavior, including fishway efficiency, swimming trajectories, swimming velocities and accelerations, resting times, and preferential resting areas.

The analysis of these data, together with the results of upcoming experiments, is expected to improve fishway design criteria in the future.

ACKNOWLEDGEMENTS

This work was supported by FEDER funds and Spanish Ministry of Economy and Competitiveness (Ministerio de Economía y Competitividad) (Ref. CGL2012-34688 and PCT-380000-2007-3). The authors would also like to thank

the Center for Hydrographic Studies of Center for Studies and Experimentation on Public Works (CEH-CEDEX), the Spanish Ministry of Education (FPU grant Ref. AP2009-2070), and the Spanish Ministry of Public Works.

REFERENCES

Ahmed, M. N. & Farag, A. A. 1997 Two-stage neural network for volume segmentation of medical images. *Pattern Recogn. Lett.* **18**, 1143–1151.

Armstrong, J. D., Bagley, P. M. & Priede, I. G. 1992 Photographic and acoustic tracking observations of the behavior of the grenadier Coryphaenoides (Nematonorus) armatus, the eel Synaphobranchus bathybius, and other abyssal demersal fish in the North Atlantic Ocean. *Mar. Biol.* **112**, 1432–1793.

Arulampalam, M. S., Maskell, S., Gordon, N. & Clapp, T. 2002 A tutorial on particle filters for online nonlinear/non-Gaussian Bayesian tracking. *IEEE Trans. Signal Process.* **50**, 174–188.

Baumgartner, L., Bettanin, M., McPherson, J., Jones, M., Zampatti, B. & Beyer, K. 2010 *Assessment of an infrared fish counter (Vaki Riverwatcher) to quantify fish migrations in the Murray-Darling Basin. Fisheries Final Report Series*. Industry & Investment NSW, Australia.

Beamish, F. W. H. 1978 Swimming capacity. In: *Fish Physiology* (W. S. Hoar & D. J. Randall, eds). Academic Press, New York, pp. 101–187.

Bermúdez, M., Puertas, J., Cea, L., Pena, L. & Balairón, L. 2010 Influence of pool geometry on the biological efficiency of vertical slot fishways. *Ecol. Eng.* **36**, 1355–1364.

Blake, R. W. 2004 Fish functional design and swimming performance. *J. Fish Biol.* **65**, 1193–1222.

Branco, P., Santos, J. M., Katopodis, C., Pinheiro, A. & Ferreira, M.T. 2013 Pool-type fishways: two different morpho-ecological cyprinid species facing plunging and streaming flows. *PLoS ONE* **8**(5), e65089.

Canny, J. 1986 A computational approach to edge detection. *IEEE Trans. Pattern Anal. Machine Intell.* **8**, 679–698.

Castro-Santos, T., Haro, A. & Walk, S. 1996 A passive integrated transponder (PIT) tag system for monitoring fishways. *Fish. Res.* **28**, 253–261.

Chambah, M., Semani, D., Renouf, A., Courtellemont, P. & Rizzi, A. 2004 Underwater color constancy enhancement of automatic live fish recognition. In: *IS&T Electronic Imaging*, SPIE, California, USA.

Cheng, H. D., Jiang, X. H., Sun, Y. & Wang, J. 2001 Color image segmentation: advances and prospects. *Pattern Recogn.* **34**, 2259–2281.

Chorda, J., Maubourguet, M. M., Roux, H., Larinier, M., Tarrade, L. & David, L. 2010 Two-dimensional free surface flow numerical model for vertical slot fishways. *J. Hydraul. Res.* **48**, 141–151.

Chuang, M.-C., Hwang, J.-N., Williams, K. & Towler, R. 2011 Automatic fish segmentation via double local thresholding for trawl-based underwater camera systems. In *18th International Conference on Image Processing (ICIP), 11–14 September*, Brussels, Belgium.

Clausen, S., Greiner, K., Andersen, O., Lie, K.-A., Schulerud, H. & Kavli, T. 2007 Automatic segmentation of overlapping fish using shape priors. In: *Scandinavian Conference on Image Analysis*, Aalborg, Denmark, pp. 11–20.

Cowx, I. G. & Welcomme, R. L. 1998 *Rehabilitation of Rivers for Fish: A Study Undertaken by the European Inland Fisheries Advisory Commission of FAO*. Fishing News Books for FAO, Oxford, UK.

Deng, Z., Richmond, C. M., Guest, G. R. & Mueller, R. P. 2004 *Study of Fish Response Using Particle Image Velocimetry and High-Speed, High-Resolution Imaging*. Technical Report, US Department of Energy, Washington, DC.

Dewar, H. & Graham, J. 1994 Studies of tropical tuna swimming performance in a large water tunnel – energetics. *J. Exp. Biol.* **192**, 13–31.

Dong, G. & Xie, M. 2005 Color clustering and learning for image segmentation based on neural networks. *IEEE Trans. Neural Netw.* **16**, 925–936.

Duarte, S., Reig, L., Oca, J. & Flos, R. 2004 Computerized imaging techniques for fish tracking in behavioral studies. In: *Aquaculture Europe'04*, European Aquaculture Society. Barcelona, Spain, pp. 310.

Gift, D. & Paulin, C. 2014 Integration of an evolutionary algorithm into an ensemble Kalman filter and a particle filter for hydrologic data assimilation. *J. Hydroinf.* **16**(1), 74–94.

Jackson, D. C., Marmulla, G., Larinier, M., Miranda, L. E. & Bernacsek, G. M. 2001 Dams, fish and fisheries. Opportunities, challenges and conflict resolution. In: *FAO Fisheries Technical Paper* (G. Marmulla, ed.). Rome, 166.

Jensen, A. & YangQuan, C. 2013 Tracking tagged fish with swarming unmanned aerial vehicles using fractional order potential fields and Kalman filtering. In: *Unmanned Aircraft Systems (ICUAS), 2013 International Conference. 28–31 May*, Atlanta, GA, pp. 1144–1149.

Kohonen, T. 1982 Self-organized formation of topologically correct feature maps. *Biol. Cybernet.* **43**, 59–69.

Lines, J. A., Tillett, R. D., Ross, L. G., Chan, D., Hockaday, S. & McFarlane, N. J. B. 2001 An automatic image-based system for estimating the mass of free-swimming fish. *Comput. Electron. Agrc.* **31**, 151–168.

Mateus, C. S. 2007 *Performance and Swimming Behaviour of the Iberian Barbel (Barbus Bocagei Steindachner, 1865) in an Experimental Pool-type Fishway Assessed by Electromyogram Telemetry*. University of Evora, Portugal.

Mitra, V., Wang, C.-J. & Banerjee, S. 2006 Lidar detection of underwater objects using a neuro-SVM-based architecture. *IEEE Trans. Neural Netw.* **17**, 717–731.

Morais, E. F., Campos, M. F. M., Padua, F. L. C. & Carceroni, R. L. 2005 Particle filter-based predictive tracking for robust fish count. In: *Brazilian Symposium on Computer Graphics*

and Image Processing (SIBGRAPI). 9–12 October, Natal, Brazil.

Ngan, S.-C. & Hu, X. 1999 Analysis of functional magnetic resonance imaging data using self-organizing mapping with spatial connectivity. *Magn. Reson. Med.* **41**, 939–946.

Petrell, R. J., Shi, X., Ward, R. K., Naiberg, A. & Savage, C. R. 1997 Determining fish size and swimming speed in cages and tanks using simple video techniques. *Aquacult. Eng.* **16**, 63–84.

Puertas, J., Pena, L. & Teijeiro, T. 2004 An experimental approach to the hydraulics of vertical slot fishways. *J. Hydraul. Eng.* **130**, 10–23.

Puertas, J., Cea, L., Bermudez, M., Pena, L., Rodriguez, A., Rabuñal, J., Balairón, L., Lara, A. & Aramburu, E. 2012 Computer application for the analysis and design of vertical slot fishways in accordance with the requirements of the target species. *Ecol. Eng.* **48**, 51–60.

Rajaratnam, N., Van der Vinne, G. & Katopodis, C. 1986 Hydraulics of vertical slot fishways. *J. Hydraul. Eng.* **112**, 909–927.

Rodriguez, A., Bermudez, M., Rabuñal, J., Puertas, J., Dorado, J. & Balairon, L. 2011 Optical fish trajectory measurement in fishways through computer vision and artificial neural networks. *J. Comput. Civil Eng.* **25**, 291–301.

Sezgin, M. & Sankur, B. 2004 Survey over image thresholding techniques and quantitative performance evaluation. *J. Electron. Imag.* **13**, 146–165.

Shortis, M. R., Ravanbakskh, M., Shaifat, F., Harvey, E. S., Mian, A., Seager, J. W., Culverhouse, P. F., Cline, D. E. & Edgington, D. R. 2013 A review of techniques for the identification and measurement of fish in underwater stereo-video image sequences. In: *PIE 8791, Videometrics, Range Imaging, and Applications XII; and Automated Visual Inspection*, Vol. 8791. Munich, Germany, pp. 87910G-87910G-10.

SIGMUR 2003 *Filtering techniques. Geography Degree. Tele Detection*. University of Murcia, Spain.

Silva, A. T., Santos, J. M., Ferreira, M. T., Pinheiro, A. N. & Katopodis, C. 2012 Passage efficiency of offset and straight orifices for upstream movements of Iberian barbel in a pool-type fishway. *River Res. Appl.* **28**, 529–542.

Spampinato, C., Chen-Burger, Y.-H., Nadarajan, G. & Fisher, R. 2008 Detecting, tracking and counting fish in low quality unconstrained underwater videos. In: *Int. Conf. on Computer Vision Theory and Applications (VISAPP). 22–25 January*, Funchal, Madiera, pp. 514–519.

Steig, T. W. & Iverson, T. K. 1998 Acoustic monitoring of salmonid density, target strength, and trajectories at two dams on the Columbia River, using a split-beam scaning system. *Fish. Res.* **35**, 43–53.

Stenger, B., Mendonca, P. R. S. & Cipolla, R. 2001 Model-based hand tracking using an unscented Kalman filter. In: *British Machine Vision Conference. 10–13 September*, Manchester, UK, pp. 63–72.

Szeliski, R. 2011 *Computer Vision: Algorithms and Applications*. Texts in Computer Science. Springer, London.

Tarrade, L., Texier, A., David, L. & Larinier, M. 2008 Topologies and measurements of turbulent flow in vertical slot fishways. *Hydrobiologia* **609**, 177–188.

Verikas, A., Malmqvist, K. & Bergman, L. 1997 Color image segmentation by modular neural networks. *Pattern Recogn. Lett.* **18**, 173–185.

Waldemark, J. 1997 An automated procedure for cluster analysis of multivariate satellite data. *Int. J. Neural Syst.* **8**, 3–15.

Weaver, C. R. 1963 Influence of water velocity upon orientation and performance of adult migrating salmonids. *Fishery Bulletin*. U.S. Fish and Wildlife Service, Washington, DC, pp. 97–121.

Webb, P. W. 1975 Hydrodynamics and energetics of fish propulsion. *J. Fish. Res. Board Can.* **190**, 1–159.

Weber, L., Goodwin, R., Li, S., Nestler, J. & Anderson, J. 2006 Application of an Eulerian-Lagrangian-Agent method (ELAM) to rank alternative designs of a juvenile fish passage facility. *J. Hydroinf.* **8**, 271–295.

Welch, G. & Bishop, G. 2006 *An Introduction to the Kalman Filter*. Department of Computer Science, University of North Carolina, Chapel Hill, NC.

Weng, J., Cohen, P. & Herniou, M. 1992 Camera calibration with distortion models and accuracy evaluation. *IEEE Trans. Pattern Anal. Mach. Intell.* **14**, 965–980.

Yilmaz, A., Javed, O. & Shah, M. 2006 Object tracking: A survey. *ACM Comput. Surv.* **38**, 45.

Yu, K. K. C., Watson, N. R. & Arrillaga, J. 2005 An adaptive Kalman filter for dynamic harmonic state estimation and harmonic injection tracking. *IEEE Trans. Power Deliv.* **20**, 1577–1584.

Yun, X. & Bachmann, E. R. 2006 Design, implementation, and experimental results of a quaternion-based Kalman filter for human body motion tracking. *IEEE Trans. Robot.* **22**, 1216–1227.

Zhang, Z. 1999 Flexible camera calibration by viewing a plane from unknown orientations. In International Conference on Computer Vision (ICCV). Kerkyra, Greece, pp. 666–673.

Zhang, H., Fritts, J. E. & Goldman, S. A. 2008 Image segmentation evaluation: A survey of unsupervised methods. *Comput. Vision Image Underst.* **110**, 260–280.

First received 28 February 2014; accepted in revised form 10 October 2014. Available online 5 November 2014